marine drugs

MDPI

Article

MARINE-INSPIRED ENZYMATIC MINERALIZATION OF DAIRY-DERIVED WHEY PROTEIN ISOLATE (WPI) HYDROGELS FOR BONE TISSUE REGENERATION

Karl Norris[1]*, Magdalena Kocot[2], Anna M. Tryba[2], Feng Chai[3], Abdullah Talari[1,4], Lorna Ashton[4], Bogdan V. Parakhonskiy[5,6], Sangram K. Samal[7], Nicholas Blanchemain[3], Elżbieta Pamuła[2] and Timothy E.L. Douglas[1,8]

[1] Engineering Department, Lancaster University, Lancaster, United Kingdom; hwbkn3@gmail.com; t.douglas@lancaster.ac.uk
[2] AGH University of Science and Technology, Faculty of Materials Science and Ceramics, Department of Biomaterials and Composites, Kraków, Poland; kocotmagda@gmail.com; amtryba@agh.edu.pl; epamula@agh.edu.pl
[3] Univ. Lille, INSERM, CHU Lille, U1008 - Controlled Drug Delivery Systems and Biomaterials, France; fchai@univ-lille2.fr; nicolas.blanchemain@univ-lille.fr
[4] Chemistry Department, Lancaster University, Lancaster, United Kingdom; a.talari@lancaster.ac.uk;l.ashton@lancaster.ac.uk
[5] Department of Biotechnology, Ghent University, Belgium; Bogdan.parakhonskiy@ugent.be
[6] Saratov State University, Russia
[7] Laboratory of Biomaterials and Regenerative Medicine for Advanced Therapies, Indian Council of Medical Research-Regional Medical Research Center, Bhubaneswar-751 023, Odisha, India; sksamalrec@gmail.com
[8] Lancaster University, Materials Science Institute (MSI), Lancaster, United Kingdom
* Correspondence: fbskn@leeds.ac.uk;

Received: date; Accepted: date; Published: date

Abstract: Whey protein isolate (WPI) is a by-product from the production of cheese and Greek yoghurt comprising β-lactoglobulin (β-lg) (75%). Hydrogels can be produced from WPI solutions through heating; hydrogels can be sterilized by autoclaving. WPI hydrogels have shown cytocompatibility and ability to enhance proliferation and osteogenic differentiation of bone-forming cells. Hence, they have promise in the area of bone tissue regeneration. In contrast to commonly used ceramic minerals for bone regeneration, a major advantage of hydrogels is the ease of their modification by incorporating biologically active substances such as enzymes. Calcium carbonate ($CaCO_3$) is the main inorganic component of the exoskeletons of marine invertebrates. Two polymorphs of $CaCO_3$, calcite and aragonite, have shown the ability to promote bone regeneration. Other authors have reported that the addition of magnesium to inorganic phases has a beneficial effect on bone-forming cell growth. In this study, we employed a biomimetic, marine-inspired approach to mineralize WPI hydrogels with an inorganic phase consisting of $CaCO_3$ (mainly calcite) and $CaCO_3$ enriched with magnesium using the calcifying enzyme urease. The novelty of this study lies in both the enzymatic mineralization of WPI hydrogels and enrichment of the mineral with magnesium. Calcium was incorporated into the mineral formed to a greater extent than magnesium. Increasing the concentration of magnesium in the mineralizatiom medium led to a reduction in the amount and crystallinity of the mineral formed. Biological studies revealed that mineralized and unmineralized hydrogels were not cytotoxic and promoted cell viability to comparable extents (approximately 74% of standard tissue culture polystyrene). The presence of magnesium in mineral formed had no adverse effect on cell viability. In short, WPI hydrogels, both unmineralized and mineralized with $CaCO_3$ and magnesium-enriched $CaCO_3$, show potential as biomaterials for bone regeneration.

Keywords: hydrogel; composite; mineralization; enzyme; bioinspired; whey protein isolate.

1. Introduction

Natural biproducts from industrial processes have tremendous biomimetic properties and are inexpensive as they are infrequently utilized. Whey protein isolate (WPI) is a by-product from the production of cheese and Greek yoghurt comprising β-lactoglobulin (β-lg) (50%) and α-lactalbumin (α-la) (20%) [1]. WPI in solution has been shown to enhance osteogenic differentiation of bone-forming cells and promote cellular proliferation [1]. It was recently discovered that hydrogels can be produced from WPI solutions, whereby gelation is achieved through heating and sterilization is achieved by autoclaving [2-4].

With regards to mechanical properties, hydrogels are relatively weak due to the high water content. However, the incorporation of a mineral phase may improve the mechanical properties and therefore promote cellular adhesion, proliferation and osteogenic differentiation [5]. In comparison to ceramic minerals, a major advantage of hydrogels is that they can be modified with ease by incorporating biologically active substances such as enzymes. Similarly, it is possible to modify and enhance properties of hydrogels by enriching the solution with a mineral phase either before or after gelation [6].

Marine invertebrates use the mineral calcium carbonate ($CaCO_3$) in their exoskeletons. $CaCO_3$ occurs naturally as three crystalline polymorphs known as calcite, aragonite and vaterite. Calcite occurs in bivalves and certain sponges, while aragonite occurs in coral and nacre, or „mother of pearl“. All three polymorphs of $CaCO_3$ may exhibit beneficial biological properties. For example, calcite is a bioactive substance that can form direct connections with bone tissue *in vivo* and could potentially strengthen fractured bone [7]. Aragonite has been employed as a biomaterial for bone regeneration and outperformed calcium phosphates [8], and when added in particle form to WPI hydrogels, has improved mechanical properties and proliferation of osteoblast-like cells [4]. Vaterite coatings have been shown to stimulate the formation of apatite upon incubation in simulated body fluid (SBF) [9]. Hence, one may hypothesize that enzymatic mineralization of WPI hydrogels with polymorphs of $CaCO_3$ will improve their biological performance *in vitro* and *in vivo*.

Several approaches to mineralize hydrogels have been tried (Gkioni et al – reference 5). The most popular approach is the addition of pre-formed ceramic particles (e.g. hydroxyapatite, bioactive glasses) during hydrogel formation. Enzymatic mineralization has certain advantages over addition of pre-formed particles. Firstly, particles are prone to aggregation, resulting in inhomogenous distribution, while enzymatic mineralization can potentially lead to a more homogeneous distribution of mineral and better integration of mineral with the hydrogel network. Secondly, the amount of pre-formed ceramic particles which can be incorporated is limited to approximately 30-50% [5], as the presence of too many particles may impede formation of the hydrogel. Using enzymatic mineralization, larger mineral contents can be achieved.

In previous work, hydrogels have been mineralized enzymatically with calcium phosphate (CaP) using alkaline phosphatase (ALP), the enzyme responsible for mineralization of bone tissue. One advantage of using urease instead of ALP is the superior thermal stability of urease at higher temperatures such as 70 °C, at which WPI hydrogels are formed.

The reaction steps of mineral precipitation using urease have been described previously [10]. Briefly, urea diffuses into the hydrogel, where it is converted under the action of urease into ammonia and bicarbonate ions. After dissociation of bicarbonate ions to hydrogen and carbonate ions, the carbonate ions react with calcium, which has also diffused into the hydrogel, to form $CaCO_3$. The hydrogen ions formed by the dissociation of the bicarbonate ions are neutralized by the ammonia, resulting in a sufficiently high pH to allow $CaCO_3$ precipitation.

Another beneficial enriching agent is magnesium, which can be found in the calcareous exoskeletons of certain marine organisms and may provide benefits to mammals [11]. Previous work has shown that the presence of magnesium in CaP has promoted adhesion and proliferation of osteoblastic cell lines [12]. During enzymatic mineralization of hydrogels with $CaCO_3$, magnesium ions can be added to the mineralization medium which may lead to an increase in cell number [13,14].

In previous work, Gellan Gum (GG) hydrogels have been mineralized with $CaCO_3$ and/or calcium magnesium carbonate by incorporation of the enzyme urease into the hydrogel network followed by incubation in a solution containing the enzyme substrate, urea, and calcium and magnesium ions [14,15].

In the following study, the enzymatic mineralization approach was extended to WPI hydrogels. WPI hydrogels were mineralized with $CaCO_3$ or magnesium-enriched $CaCO_3$ via enzymatic mineralization with urease and incubation in solutions containing calcium and magnesium ions. The novelty of this study lies in both the enzymatic mineralization of WPI hydrogels and enrichment of the mineral with magnesium. It was thus demonstrated that urease retained activity after incorporation into WPI hydrogels, which involved gelation at 70 °C. Three different Ca:Mg concentration ratios were compared. The resulting hydrogels were subjected to physicochemical, morphological and biological characterization to examine the influence of Ca:Mg ratio.

2. Results

Influence of mineralization medium on extent and elemental composition of mineral formed

We aimed to enhance the properties of WPI hydrogels by mineralization with $CaCO_3$ or magnesium-enriched $CaCO_3$. The effects of Ca^{2+} and Mg^{2+} content of the mineralization media on extent of mineral formed were investigated. As expected, a dose dependent effect was observed depending in which medium the urease WPI hydrogel was incubated (Table 1, Fig. 1A and B). Notably, WPI hydrogels containing urease were able to retain higher amounts of Ca^{2+} and Mg^{2+} than control hydrogels, suggesting a greater extent of mineralization. When WPI hydrogels containing urease were incubated with calcium and magnesium in equimolar concentrations (WPI_U_MC), calcium content was five-fold that of magnesium, indicating that calcium was preferentially incorporated into the hydrated polymer. The increase in dry mass as a result of enzymatic mineralization was highest for hydrogels incubated in calcium only (WPI_U_MA) (Fig. 1C).

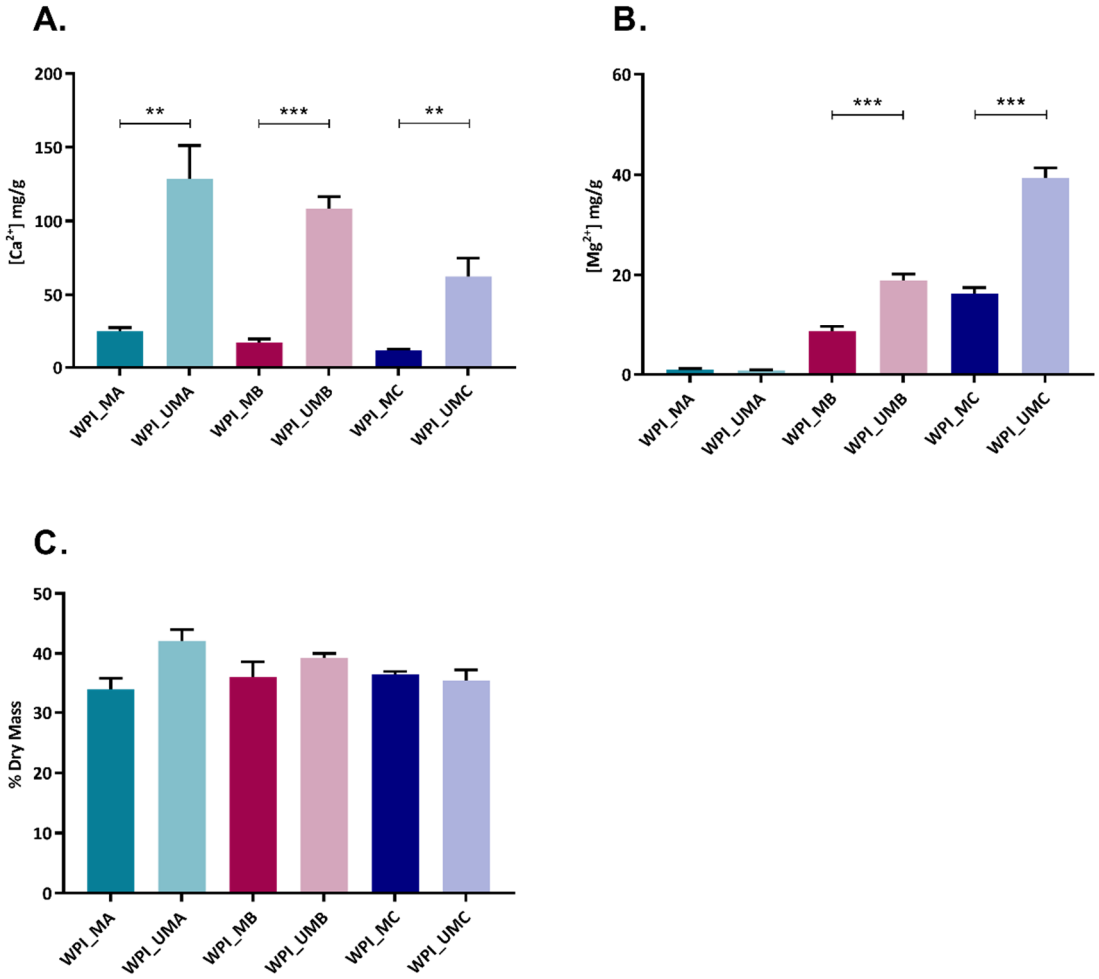

Figure 1 Mass of elemental calcium (A) and magnesium (B) per unit mass of hydrogel and dry mass percentage (C) of WPI hydrogels without urease (WPI) and with urease (WPI_U) incubated in different media: MA, MB, MC, n = 3, * $p<0.05$, ** $p<0.01$, *** $p<0.001$.

Physicochemical characterization of mineral formed by FTIR, Raman, XRD and SEM

FTIR spectra (Fig. 3A) of urease-free hydrogels indicated characteristic bands for WPI at 1650, 1570 and 1350-1200 cm^{-1} [16]. In contrast, hydrogels containing urease showed bands characteristic of calcium carbonate. There was a broad band at 1400 cm^{-1}, which is indicative of calcite and corresponds to v_3 antisymmetric stretching of carbonate group [17]. Moreover, a band at approximately 1500 cm^{-1} was detected, which might indicate the presence of vaterite. This band was more intense in WPI_U_MA than in samples incubated in MB and MC. A band at approximately 1080 cm^{-1} was also observed in all hydrogels with urease and might indicate that vaterite was formed within these hydrogels [18]. In all hydrogels with urease, bands at 870 and 715 cm^{-1} correspond to v_2 out-of-plane bending and v_4 in-plane bending, respectively. These bands are characteristic for calcite [17]. These results show strong evidence that, in WPI hydrogels containing urease, the minerals calcite and vaterite were formed.

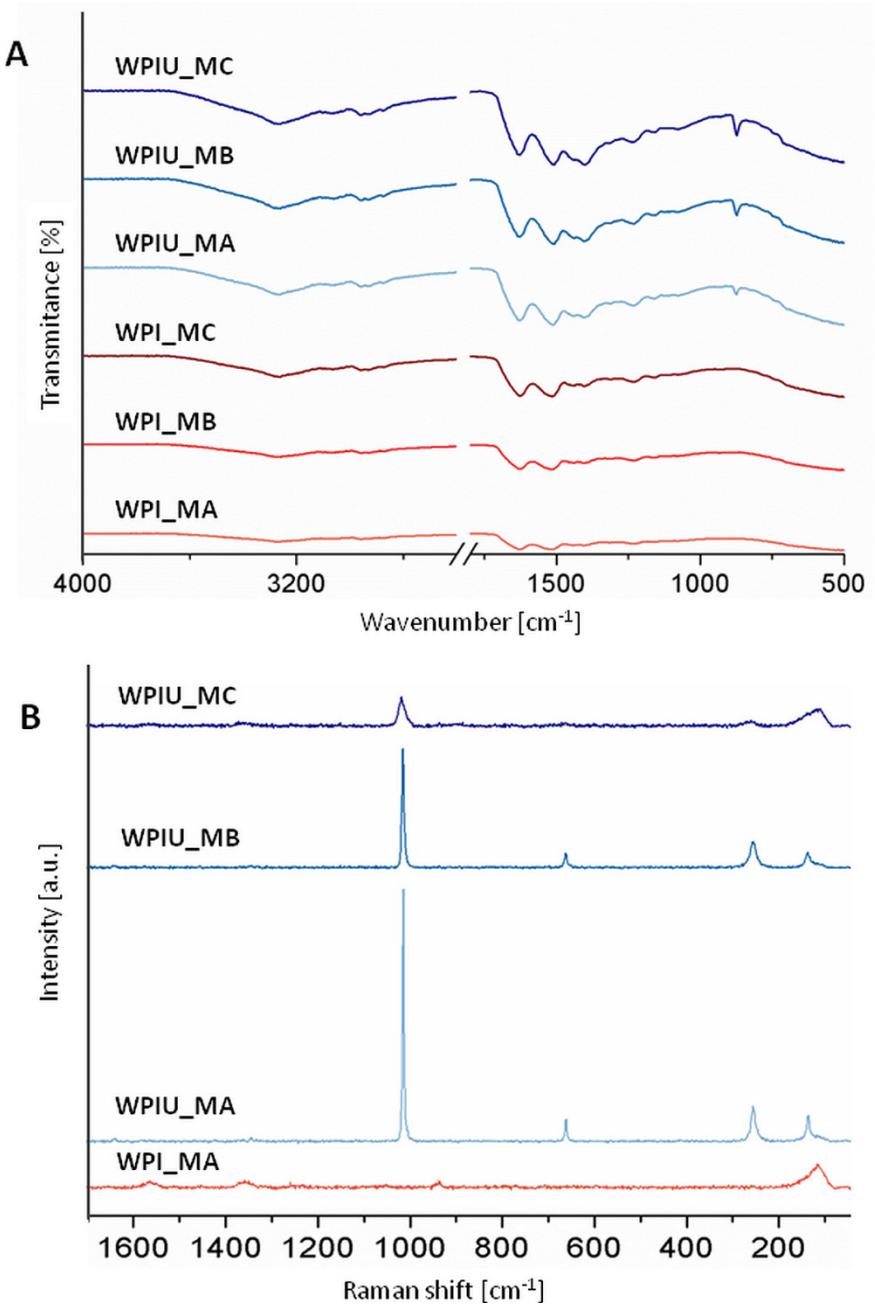

Figure 2 FTIR (A) and Raman spectra (B) of WPI hydrogels without and with urease WPI_U incubated in different media: MA, MB, MC.

Raman spectra of control WPI_MA hydrogels (Fig. 2 B) showed bands at 1658 cm^{-1} and 1453 cm^{-1}, which are associated with amide I and CH_2 bending, respectively [19]. There were also bands at approximately 1000 cm^{-1} relating to phenylalanine [20,21]. Bands typical for $CaCO_3$ were not observed. In contrast, WPI_U_MA and WPI_U_MB showed intense bands at 1085 cm^{-1}, which are typical for $CaCO_3$ and correspond to v_1 symmetric stretching [22]. Raman bands were also observed at 711 cm^{-1} relating to v_4 in-plane stretching and both hydrogels showed bands at 281 cm^{-1} and 154 cm^{-1} consistent with lattice vibration modes [22]. Sharp peaks in WPI_U_MA and WPI_U_MB were indicative of crystalline structure. In WPI_U_MC Raman bands at 1085 cm^{-1} were broader and less intense, suggesting increased amorphicity and thus incorporation of magnesium in the calcite lattice. It was found that increased magnesium concentration reduced the crystallinity of $CaCO_3$. This

observation was confirmed by two other bands typical for calcite (at 281 cm^{-1} and 154 cm^{-1}), which were also broader in WPI_U_MC than in WPI_U_MA and WPI_U_MB [17,23,24]. The decrease in intensity and band sharpness in the order WPIU_MA > WPIU_MB > WPIU_MC suggests a decrease in crystallinity in the same order.

XRD diffractograms of control samples (urease-free hydrogels) displayed a peak at a 2 theta value of approximately 19.5, which is a characteristic peak for WPI (Fig. 3) [20]. However, in WPI hydrogels with urease (WPI_U) this peak was less intense, which might suggest that the proportion of mineral present in this sample was higher than the proportion of WPI. Minerals formed in all WPI hydrogels containing urease, displaying peaks at 23.2, 29.5, 36.1, 39.5, 43.3, 47.7, 48.6 and 57.5, which are characteristic for calcite [13,25]. In addition, WPI_U_MA hydrogels displayed peaks characteristic for vaterite at 24.9, 27.0 and 32.8 [26]. A peak near 30 degrees in WPI_U_MC hydrogels may indicate the presence of calcium magnesium carbonate. XRD may be also used to identify the degree of crystallinity of material. Crystalline materials show sharp peaks whereas amorphous produce a broad background pattern. Therefore, it could be concluded that WPI hydrogels with urease incubated in media MA and MB (WPIU_MA and WPIU_MB) are crystalline, as indicated by sharp peaks [13,25]. The lower intensity and sharpness of peaks of hydrogels incubated in medium MC (WPI_U_MC) suggests lower crystallinity.

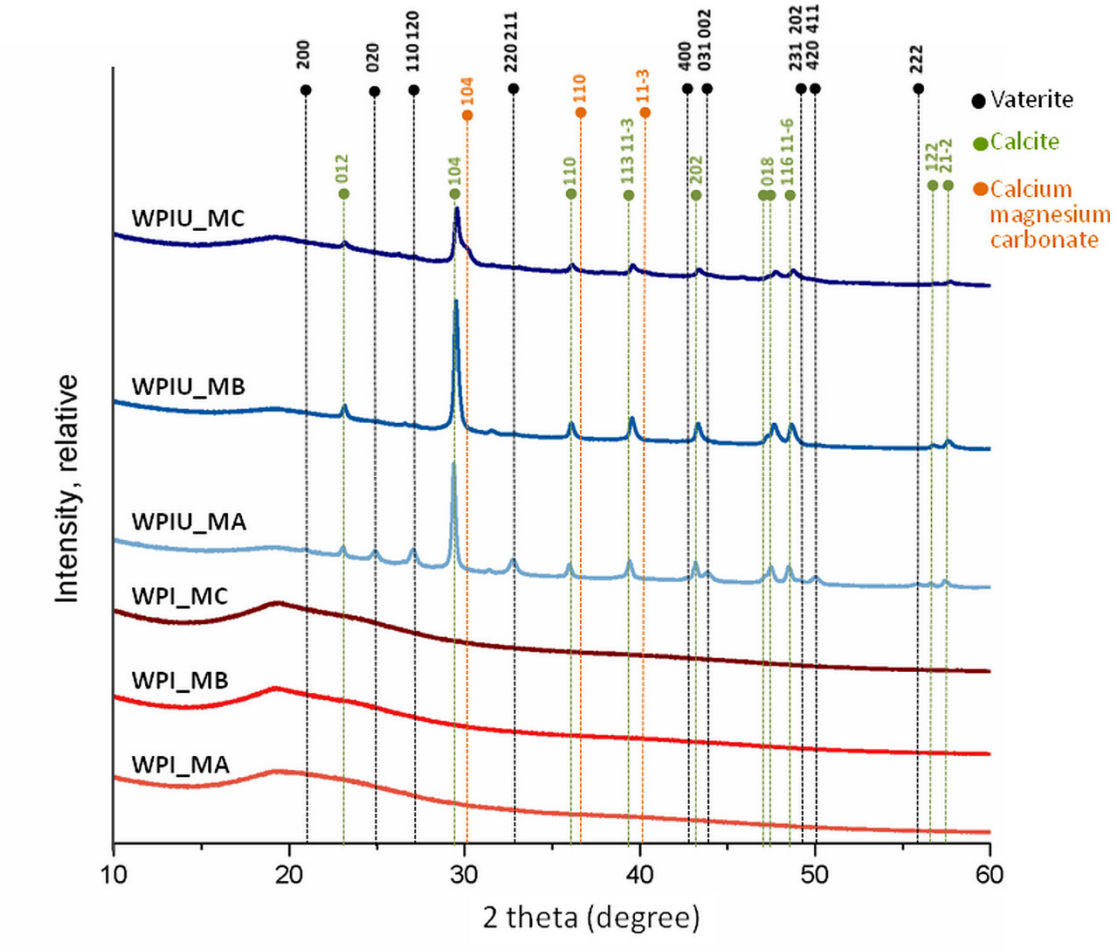

Figure 3 XRD diffractograms of WPI hydrogels incubated in different media MA, MB and MC

The morphology of the different WPI hydrogels was studied by SEM (Figure 4). As expected, WPI hydrogels without urease displayed surfaces devoid of mineral deposits (Figure 4A-C). The surface of hydrogels incubated in medium MA was smooth, whereas hydrogels incubated in medium MB and MC had some deposits on the surface, which might have been polymer residues. In contrast,

181 WPI hydrogels containing urease displayed microstructures rich in mineral deposits (Figure 4D-L).
182 In mineralized hydrogels incubated in medium MA (WPI_U_MA), some porous cube-like deposits
183 typical for calcite and spherical deposits typical for vaterite were observed [27,28]. Moreover, some
184 undefined elongated, rod-like deposits were also detected on the surface of hydrogels incubated in
185 medium MA. Cuboid deposits typical for calcite were also observed in WPI hydrogels incubated in
186 media containing magnesium (MB and MC). However, there were also some undefined deposits in
187 samples incubated in medium with the highest concentration of magnesium (MC), which were not
188 described in previous studies [14,27]. This finding suggests a lower degree of crystallinity of the
189 mineral formed in such samples (WPI_U_MC). In mineralized hydrogels incubated in medium MB
190 (WPI_U_MB), besides rhombohedral crystals of calcite, there were also rod-like crystals covered with
191 spherical deposits. Plate-like deposits, which were reported in previous work on GG hydrogels and
192 are characteristic of hydromagnesite, were not observed in WPI hydrogels [14].
193
194

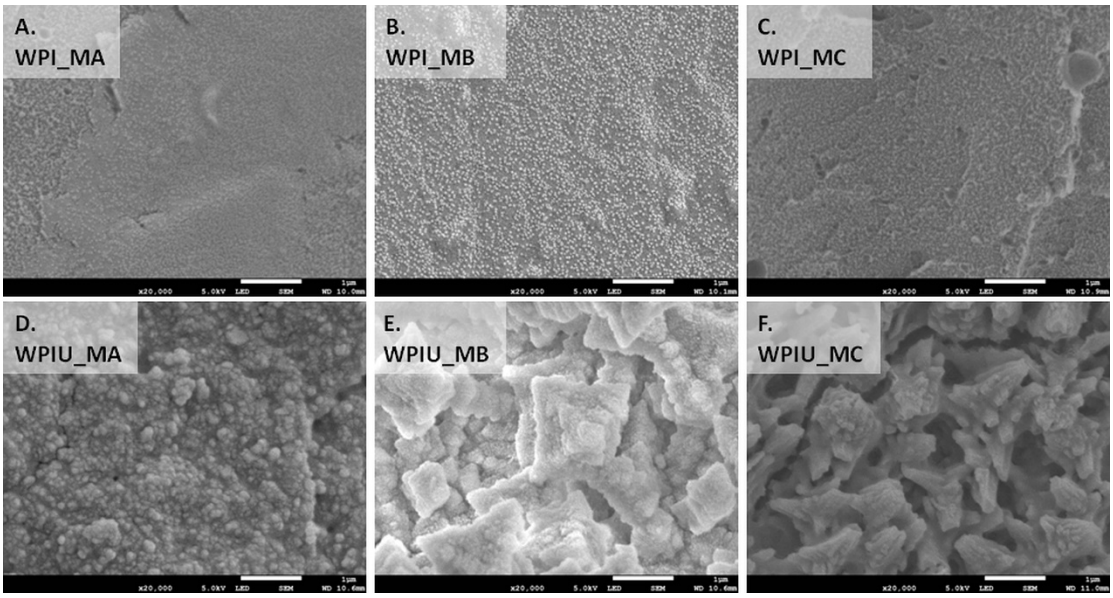

195

196 Figure 4 SEM images of WPI and WPI_U hydrogels incubated in medium MA (A, D), MB (B, E) and
197 MC (C, F). Scale bar is representative of 1 μm (A, B, C) and 10 μm (D, E, F)

198 *Cytotoxicity studies and release of Ca and Mg into cell culture medium*

199 Cell viability experiments utilizing the AlamarBlue assay (Fig. 5) indicated that none of the
200 hydrogels were immediately cytotoxic. Cells were viable following 24 hours incubation on the WPI
201 hydrogels. Interestingly, cell viability increased on WPI hydrogels which lacked urease where the
202 calcium and magnesium concentrations decreased and increased, respectively (WPI_MA vs WPI_MB
203 vs WPI_MC). In contrast, viability remained similar for all WPI hydrogels mineralized with urease,
204 independently of the mineralization medium used. For the most part, cell viability remained
205 comparable after 72 hours, indicating that the cells were able to adhere and remain viable.

206

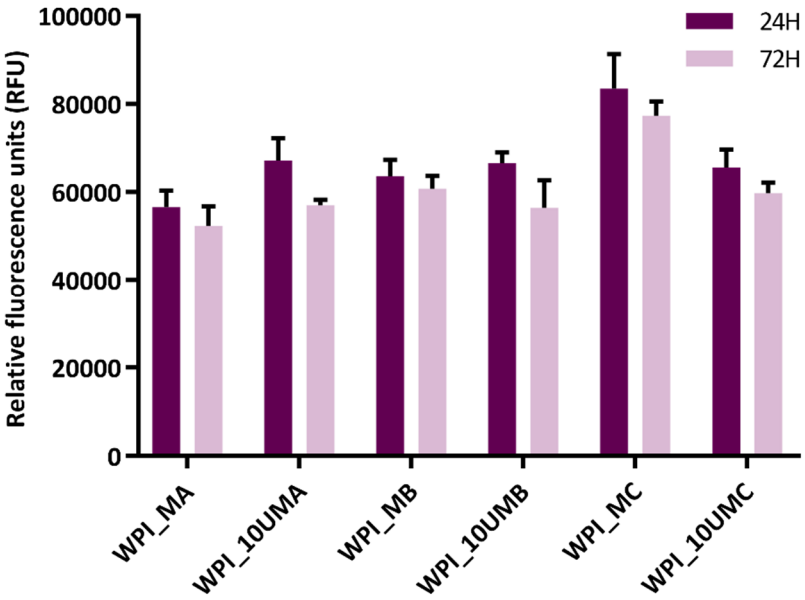

207

208 Figure 5. Cell viability of mouse osteoblast (MC3T3-E1 cells) seeded onto hydrogels over 24 and 72
209 hours. Background fluorescence of AlamarBlue and cell culture media was subtracted from each
210 experimental hydrogel. n = 3, error bars are representative of SD.

211

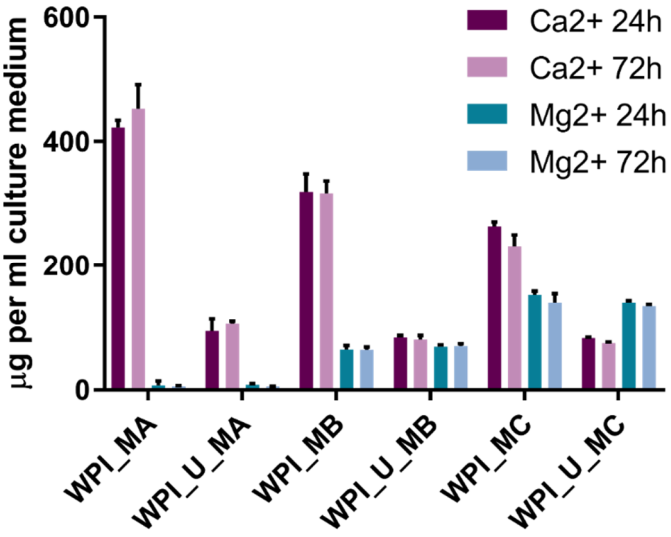

212

213 Figure 6. Concentrations of elemental Ca and Mg in hydrogel extracts after 24 h and 72 h. n = 3, error
214 bars show standard deviation.

215 The results of measurements of elemental Ca and Mg in extraction medium (Fig. 6) revealed that
216 considerably more Ca and Mg were released from hydrogels which did not contain urease, i.e. which
217 were unmineralized. One explanation may be the presence of residual mineralization medium
218 containing Ca and Mg in the hydrogels, allowing these ions to diffuse out more easily from
219 unmineralized samples. In mineralized samples, taking into account the lower amount of Mg present

compared to Ca (Table 2), Mg was preferentially released. It was noticeable that the concentrations present in the extraction medium were similar after 24 h and 72 h. This suggests that practically all Ca and Mg release takes place within the first 24 h.

3. Discussion

Enzymatic mineralization of WPI hydrogels was demonstrated directly by FTIR and Raman spectra (Fig. 2), XRD diffractograms (Fig. 3), SEM images (Fig. 4), and indirectly by ICP-OES quantification of elemental magnesium and calcium and measurement of dry mass percentage (Fig. 1).

The amount of mineral formed was highest when the mineralization medium contained only calcium, i.e. in sample group WPI_U_MA. Furthermore, when both calcium and magnesium were present in the mineralization medium, calcium was preferentially incorporated into mineral formed. These results were consistent with previous studies on urease-mediated mineralization of GG hydrogels [14]. This effect was also observed for CaP formation and can be explained by the mechanism proposed by Martin and Brown [29]. Accordingly, magnesium ions in solution are more hydrated than calcium ions, thus undergo dehydration more slowly, which results in their adsorption on $CaCO_3$. Subsequently, they are not included in the carbonate mineral and remain on the surface. As a result, the total amount of magnesium the mineral formed is lower.

Marine research on exoskeletons of marine invertebrates mineralized with $CaCO_3$ has revealed similar effects. In studies in which the effect of the Mg:Ca elemental ratio in seawater on the incorporation of magnesium into marine invertebrate exoskeletons and non-skeletal precipitation was investigated [30,31], preferential incorporation of calcium was reported.

A decrease of crystallinity in the order WPIU_MA > WPIU_MB > WPIU_MC was observed using Raman spectroscopy (Fig. 2B), XRD (Fig. 3) and SEM (Fig. 4). This can also be explained by the mechanism proposed by Martin and Brown (see above), whereby magnesium ions dehydrate more slowly and hence are not included in the carbonate mineral and remain on the surface [29]. XRD results suggested that small amounts of calcium magnesium carbonate may have formed in WPIU_MC samples (Figure 3). Raz et al. (2000) proposed that calcium magnesium carbonate forms via an amorphous precursor phase, into which hydrated magnesium ions can be more easily incorporated in the amorphous precursor phase and hence are more likely to be incorporation into the final, more crystalline calcium magnesium carbonate phase [32]. Furthermore, magnesium may stabilize the amorphous precursor phase; magnesium has been reported to 'poison' calcite formation by binding to the surface of calcite nuclei and inhibiting further crystal growth as a result of its hydration [33].

SEM images (Fig. 4) revealed differences in the morphologies of mineral deposits formed in WPI hydrogels in this study and those formed in GG hydrogels in previous work [14]. Hydrogels are 3D cross-linked polymer networks with entrapped water. The mechanism of WPI hydrogel formation at elevated temperature and pressure involves denaturation of its main component β-lg, leading to unfolding of the molecule and the formation of disulphide bonds between β-lg molecules and the formation of a 3D cross-linked network [34].

Differences between the structures of WPI hydrogels and GG hydrogels may influences the type of mineral formed. The concentration of polymer in WPI hydrogels in this study (50% (w/v)) is much higher than in the GG hydrogels used in previous work (0.7% (w/v)) [10,14,15]. A higher concentration of polymer would lead to smaller pores in the polymer network. In turn, this would hinder diffusion of mineralization medium through the hydrogel which would lower the amount of mineral formed. Another consequence of small pores is hindrance of the formation of large crystals. Different degrees of compactness of the mineralized hydrogels were observed (Figure 4D, E, F), which may be due to the differences in the sizes of the mineral deposits. A higher concentration of polymer might however promote mineral formation; diffusion of enzyme out of the hydrogel would be impeded, and also more polymer chains mean more potential binding sites for calcium or carbonate ions which may serve as nucleation sites for crystal growth.

There is no obvious correlation between amount of Ca and Mg released (Fig. 6) and cell proliferation (Fig. 5). This demonstrates that the amounts of Ca and Mg released are non-cytotoxic and may be considered harmless. Ca concentrations of 10 mM and above have been reported to be toxic for osteoblasts, while concentrations in the range 2-4 mM have been reported to be beneficial for proliferation [35]. The Ca (and Mg) concentrations in cell culture media are in the range 0-10 mM (Fig. 6), however no obvious positive effect was observed. It is to be expected that protein is released from WPI hydrogels; one may speculate that the released protein may be binding Ca and Mg and hindering any stimulatory effect of these ions.

Previous work on GG hydrogels mineralized with calcium and magnesium carbonates by enzymatic mineralization demonstrated that hydrogels mineralized with calcite improved the adhesion and proliferation of osteoblast-like MC3T3-E1 cells, and that hydrogels mineralized with calcite containing small amounts of magnesium had no appreciable negative effect [14]. Similarly, a previous study on GG hydrogels mineralized with calcium and magnesium carbonates by alternate soaking in solutions of calcium/magnesium and carbonate ions also demonstrated comparable proliferation and differentiation of osteoblast-like MC3T3-E1 cells on hydrogels mineralized with predominantly calcite and vaterite and those mineralized with predominantly calcite and vaterite containing small amounts of magnesium [15].

The results of this study suggest that magnesium as a dopant of $CaCO_3$ does not provide an appreciable positive biological effect on cell viability, in contrast to reports of a positive effect of magnesium as a dopant of CaP. The reasons for this remain unclear and are outside the scope of this work. In this study, no appreciable effect of mineralization on swelling was observed. However, such effects are worthy of investigation in future work.

4. Materials and Methods

Production of urease WPI hydrogels containing urease

WPI hydrogels were produced as previously described [2-4]. Briefly, WPI powder (Davisco, USA) was added to ddH_2O for a final concentration of 50% (w/v). The solution was incubated in an ultrasonic bath for 30 minutes to ensure the powder had fully dissolved. Urease extracted from Canavalia ensiformis (Sigma Aldrich, U1500) was added to WPI solution at a concentration of 10 mg urease/ml solution prior to the solution being heated to 70°C for 8 min for gelation.

Mineralization of urease WPI hydrogels

The urease WPI hydrogels were mineralized using three different media at room temperature over 7 days. In these media, the concentration of urea (0.17M) was kept constant whilst the ratio of $CaCl_2$:$MgCl_2$ was varied (Table 1). Unmineralized control samples were prepared in a similar fashion by incubating urease-free WPI hydrogels in the mineralization media.

Table 1 Mineralization media composition

Medium	**Concentration (mol/dm³)**			**Ratio**
	$CaCl_2$	$MgCl_2$	Urea	
MA	0.2700	0	0.1700	1:0
MB	0.2025	0.0675	0.1700	0.75:0.25
MC	0.1350	0.1350	0.1700	0.5:0.5

Determinination of mineral formation and elemental composition

To assess the extent of mineral formation, the samples were dried at 60 °C for 48 hours. Samples were weighed before and after the drying process to calculate the dry mass percentage, or (weight

after drying/weight before drying) x 100%, which the mass percentage attributable to polymer and mineral and not water and serves as a measure of extent of mineralization.

Inductively coupled plasma optical emission spectroscopy (ICP-OES) was used to determine the calcium and magnesium content of samples using a 5100 Synchronous Vertical Dual View spectrometer (Agilent, Cheadle, UK). Prior to analysis, solid samples were dried and ground before being diluted in 1 % nitric acid and diluted 10-fold. No additional steps were necessary for liquid samples (cell culture medium), which were diluted in 1 % nitric acid immediately.

Physiochemical and morphological characterisation: Raman, XRD, SEM, FTIR

Samples were dried at 60 °C for 48 hours prior to analysis. Raman spectra were collected using a confocal Raman system (InVia, Renishaw plc, Wotton-Under edge, UK) equipped with a near infrared laser. A laser power of ~15 mW was used to prevent any damage to the samples. Spectral collection exposure time was set to 1 second with one acquisition. Spectra were collected from each sample over the spectral range of 60-1800 cm^{-1}. Pre-processing such as baseline correction was carried out using Wire 4.0 software (Renishaw plc, Wotton-Under edge, UK).

X-ray diffraction (XRD) measurements were performed with Rigaku, SmartLab 9kW with DteX-250 detector and Cu rotating anode source (Rigaku, Tokyo, Japan). Diffractometer was set to 45 kV and 200 mA. 5 degree soller slits and 2 theta scans in Bragg Brentano configuration were used.

Morphological characterization of hydrogels was performed using scanning electron microscopy (SEM). Firstly, samples were coated with a 9 nm layer of gold for 3 min at 20 mA and $1x10^{-1}$ mBar using a Quorum Q150RES sputter coater (Quorum Technologies Ltd, Lewes, UK). SEM analysis was performed using secondary electron detector JSM-7800F (Jeol UK Ltd., Welvyn Garden City). Images were acquired with an accelerating voltage of 5 kV at a working distance of about 10 mm.

The chemical structure of samples was examined using Fourier transform infrared spectroscopy (FTIR) (Agilent Technology, Cheadle, UK) in Attenuated Total Reflectance (ATR) mode. Spectra were collected in the 500 - 4000 cm^{-1} spectral range with a resolution of 4 cm^{-1} and an average of 8 scans.

Cell culture and cell viability and release of calcium and magnesium from hydrogels into cell culture medium

The mouse osteoblast MC3T3-E1 cell line (ATCC® CRL-2594™, USA) was routinely cultured in MEM-α medium supplemented with 10% FBS and incubated in a humidified 5% CO_2 environment at 37°C. Once 80% confluent, cells were trypsinized and used for cytotoxicity testing. Cell tests were carried out in accordance with the International Organization for Standardization (ISO) norm ISO 10993-5.

In 96 well polystyrene plates, 4 x 10^3 MC3T3-E1 cells were seeded on WPI hydrogels and incubated for 24 hours to allow the cells to adhere. MC3T3-E1 seeded WPI hydrogels were washed with PBS (pH 7.4) before AlamarBlue (10% in media) was added and allowed to incubate for 2 hours. Fluorescence analysis was performed using an excitation wavelength of 530 nm and an emission wavelength of 590 nm. Controls lacking cells were used to determine background fluorescence which was subsequently subtracted from cell viability results. Cell viability was measured after 24 h and 72 h.

To study release of calcium and magnesium, WPI hydrogels were incubated for 24 h or 72 h in cell culture medium under sterile conditions in the absence of cells. Calcium and magnesium concentrations in media were determined using ICP-OES as described above

Statistical analyses

Student's t-test was applied to determine statistical significance using Excel software. The results of average weight, dry mass percentage, calcium and magnesium concentration and biological tests

were analyzed. A two-tailed unpaired t-test with 95%, 99% and 99.9% confidence interval was considered statistically significant if $p < 0.05$ (*), $p < 0.01$ (**) and $p < 0.001$ (***).

5. Conclusions

WPI hydrogels were enzymatically mineralized with an inorganic phase consisting of $CaCO_3$ or magnesium-enriched $CaCO_3$. Calcium was incorporated into the mineral formed to a greater extent than magnesium. Increasing the concentration of magnesium in the mineralization medium led to reduction of mineral formed. These observations were confirmed by dry mass percentage and ICP-OES. Moreover, increasing the amount of magnesium in medium resulted in less crystalline structure of mineral formed in hydrogels as shown by XRD and Raman spectroscopy results. The type of the carbonate phase detected in all hydrogels with urease was mainly calcite, which was confirmed by SEM morphology observation, XRD and FTIR analysis. There were also some vaterite deposits detected in all hydrogels mineralized by urease. XRD analysis showed that in hydrogels incubated in mineralization medium MC with equimolar concentrations of calcium and magnesium, some calcium magnesium carbonate was also present. Biological studies revealed that hydrogels were not cytotoxic. Hydrogels mineralized by urease had similar cell viability, which amounted to 74%. The presence of magnesium in mineral formed did not promote or inhibit cell metabolic activity.

Further work should focus on biological studies concerning cell differentiation and in vivo implantation in order to determine the influence of $CaCO_3$ and magnesium-enriched $CaCO_3$ on bone tissue regeneration.

Author Contributions: Conceptualization, T.E.L.D, E.P, and A.M.T.; formal analysis, T.E.L.D, M.K, A.T, L.A, F.C, N.B, B.V.P, S.K.S, K.N; investigation, T.E.L.D, M.K, A.T, L.A, F.C, N.B, B.V.P, S.K.S; writing—original draft preparation, T.E.L.D, M.K, K.N; writing—review and editing, T.E.L.D, K.N; project administration, T.E.L.D; funding acquisition, T.E.L.D

Funding: This research was funded by N8 Agrifood pump-priming grant „Food2Bone" (K.N., T.E.L.D.). The British Council is thanked for financial support in the framework of the grant "Advanced biomaterials to combat cancer" (2019-RLWK11-10353).

Acknowledgments: Sara Baldock and David Rochester (both Lancaster University, United Kingdom) are thanked for excellent technical assistance.

Conflicts of Interest: The authors declare no conflict of interest.

References

1. Douglas, T.E.L.; Vandrovcova, M.; Krocilova, N.; Keppler, J.K.; Zarubova, J.; Skirtach, A.G.; Bacakova, L. Application of whey protein isolate in bone regeneration: Effects on growth and osteogenic differentiation of bone-forming cells. *J Dairy Sci* **2018**, *101*, 28-36, doi:10.3168/jds.2017-13119.
2. Dziadek, M.; Kudlackova, R.; Zima, A.; Slosarczyk, A.; Ziabka, M.; Jelen, P.; Shkarina, S.; Cecilia, A.; Zuber, M.; Baumbach, T. Novel multicomponent organic–inorganic WPI/gelatin/CaP hydrogel composites for bone tissue engineering. *Journal of Biomedical Materials Research Part A* **2019**, *107*, 2479-2491.
3. Dziadek, M.; Douglas, T.E.; Dziadek, K.; Zagrajczuk, B.; Serafim, A.; Stancu, I.-C.; Cholewa-Kowalska, K. Novel whey protein isolate-based highly porous scaffolds modified with therapeutic ion-releasing bioactive glasses. *Materials Letters* **2020**, *261*, 127115.
4. Gupta, D.; Kocot, M.; Tryba, A.M.; Serafim, A.; Stancu, I.C.; Jaegermann, Z.; Pamuła, E.; Reilly, G.C.; Douglas, T.E. Novel naturally derived whey protein isolate and aragonite biocomposite hydrogels have potential for bone regeneration. *Materials & Design* **2020**, *188*, 108408.
5. Gkioni, K.; Leeuwenburgh, S.C.; Douglas, T.E.; Mikos, A.G.; Jansen, J.A. Mineralization of hydrogels for bone regeneration. *Tissue Eng Part B Rev* **2010**, *16*, 577-585, doi:10.1089/ten.TEB.2010.0462.

6. Douglas, T.E.; Wlodarczyk, M.; Pamula, E.; Declercq, H.A.; de Mulder, E.L.; Bucko, M.M.; Balcaen, L.; Vanhaecke, F.; Cornelissen, R.; Dubruel, P., et al. Enzymatic mineralization of gellan gum hydrogel for bone tissue-engineering applications and its enhancement by polydopamine. *J Tissue Eng Regen Med* **2014**, *8*, 906-918, doi:10.1002/term.1616.
7. Fujita, Y.; Yamamuro, T.; Nakamura, T.; Kotani, S.; Ohtsuki, C.; Kokubo, T. The bonding behavior of calcite to bone. *J Biomed Mater Res* **1991**, *25*, 991-1003, doi:10.1002/jbm.820250806.
8. Viateau, V.; Manassero, M.; Sensebe, L.; Langonne, A.; Marchat, D.; Logeart-Avramoglou, D.; Petite, H.; Bensidhoum, M. Comparative study of the osteogenic ability of four different ceramic constructs in an ectopic large animal model. *J Tissue Eng Regen Med* **2016**, *10*, E177-187, doi:10.1002/term.1782.
9. Maeda, H.; Maquet, V.; Kasuga, T.; Chen, Q.Z.; Roether, J.A.; Boccaccini, A.R. Vaterite deposition on biodegradable polymer foam scaffolds for inducing bone-like hydroxycarbonate apatite coatings. *J Mater Sci Mater Med* **2007**, *18*, 2269-2273, doi:10.1007/s10856-007-3108-4.
10. Lopez-Heredia, M.A.; Łapa, A.; Mendes, A.C.; Balcaen, L.; Samal, S.K.; Chai, F.; Van der Voort, P.; Stevens, C.V.; Parakhonskiy, B.V.; Chronakis, I.S. Bioinspired, biomimetic, double-enzymatic mineralization of hydrogels for bone regeneration with calcium carbonate. *Materials Letters* **2017**, *190*, 13-16.
11. Borzęcka-Prokop, B.; Wesełucha-Birczyńska, A.; Koszowska, E. MicroRaman, PXRD, EDS and microscopic investigation of magnesium calcite biomineral phases. The case of sea urchin biominerals. *Journal of molecular structure* **2007**, *828*, 80-90.
12. Douglas, T.E.; Krawczyk, G.; Pamula, E.; Declercq, H.A.; Schaubroeck, D.; Bucko, M.M.; Balcaen, L.; Van Der Voort, P.; Bliznuk, V.; van den Vreken, N.M., et al. Generation of composites for bone tissue-engineering applications consisting of gellan gum hydrogels mineralized with calcium and magnesium phosphate phases by enzymatic means. *J Tissue Eng Regen Med* **2016**, *10*, 938-954, doi:10.1002/term.1875.
13. Douglas, T.E.; Lapa, A.; Reczynska, K.; Krok-Borkowicz, M.; Pietryga, K.; Samal, S.K.; Declercq, H.A.; Schaubroeck, D.; Boone, M.; Van der Voort, P., et al. Novel injectable, self-gelling hydrogel-microparticle composites for bone regeneration consisting of gellan gum and calcium and magnesium carbonate microparticles. *Biomed Mater* **2016**, *11*, 065011, doi:10.1088/1748-6041/11/6/065011.
14. Douglas, T.E.L.; Lapa, A.; Samal, S.K.; Declercq, H.A.; Schaubroeck, D.; Mendes, A.C.; der Voort, P.V.; Dokupil, A.; Plis, A.; De Schamphelaere, K., et al. Enzymatic, urease-mediated mineralization of gellan gum hydrogel with calcium carbonate, magnesium-enriched calcium carbonate and magnesium carbonate for bone regeneration applications. *J Tissue Eng Regen Med* **2017**, *11*, 3556-3566, doi:10.1002/term.2273.
15. Lopez-Heredia, M.A.; Lapa, A.; Reczynska, K.; Pietryga, K.; Balcaen, L.; Mendes, A.C.; Schaubroeck, D.; Van Der Voort, P.; Dokupil, A.; Plis, A., et al. Mineralization of gellan gum hydrogels with calcium and magnesium carbonates by alternate soaking in solutions of calcium/magnesium and carbonate ion solutions. *J Tissue Eng Regen Med* **2018**, *12*, 1825-1834, doi:10.1002/term.2675.
16. Geara, C. Study of the gelation of whey protein isolate by FTIR spectroscopy and rheological measurements. McGill University, 1999.
17. Gunasekaran, S.; Anbalagan, G.; Pandi, S. Raman and infrared spectra of carbonates of calcite structure. *Journal of Raman Spectroscopy: An International Journal for Original Work in all Aspects of Raman Spectroscopy, Including Higher Order Processes, and also Brillouin and Rayleigh Scattering* **2006**, *37*, 892-899.
18. Sato, M.; Matsuda, S. Structure of vaterite and infrared spectra. *Zeitschrift fur Kristallographie* **1969**, *129*, 405-410.

19. Alizadeh-Pasdar, N.; Nakai, S.; Li-Chan, E.C. Principal component similarity analysis of Raman spectra to study the effects of pH, heating, and κ-carrageenan on whey protein structure. *Journal of agricultural and food chemistry* **2002**, *50*, 6042-6052.
20. Zhang, S.; Zhang, Z.; Lin, M.; Vardhanabhuti, B. Raman spectroscopic characterization of structural changes in heated whey protein isolate upon soluble complex formation with pectin at near neutral pH. *Journal of agricultural and food chemistry* **2012**, *60*, 12029-12035.
21. Nonaka, M.; Li-Chan, E.; Nakai, S. Raman spectroscopic study of thermally induced gelation of whey proteins. *Journal of Agricultural and Food Chemistry* **1993**, *41*, 1176-1181.
22. Farmer, V.C. *Infrared spectra of minerals*; Mineralogical society: 1974.
23. Douglas, T.E.; Sobczyk, K.; Łapa, A.; Włodarczyk, K.; Brackman, G.; Vidiasheva, I.; Reczyńska, K.; Pietryga, K.; Schaubroeck, D.; Bliznuk, V. Ca: Mg: Zn: CO3 and Ca: Mg: CO3—tri-and bi-elemental carbonate microparticles for novel injectable self-gelling hydrogel–microparticle composites for tissue regeneration. *Biomedical Materials* **2017**, *12*, 025015.
24. Bischoff, W.D.; Sharma, S.K.; MacKenzie, F.T. Carbonate ion disorder in synthetic and biogenic magnesian calcites: a Raman spectral study. *American Mineralogist* **1985**, *70*, 581-589.
25. Landi, E.; Logroscino, G.; Proietti, L.; Tampieri, A.; Sandri, M.; Sprio, S. Biomimetic Mg-substituted hydroxyapatite: from synthesis to in vivo behaviour. *Journal of Materials Science: Materials in Medicine* **2008**, *19*, 239-247.
26. Chen, Z.; Xin, M.; Li, M.; Xu, J.; Li, X.; Chen, X. Biomimetic synthesis of coexistence of vaterite-calcite phases controlled by histidine-grafted-chitosan. *Journal of crystal growth* **2014**, *404*, 107-115.
27. Bermanec, V.; Posilović, H.; Žigovečki Gobac, Ž. Identification of biogenetic calcite and aragonite using SEM. *Geologia Croatica* **2009**, *62*, 0-0.
28. Yang, D.; Qi, L.; Ma, J. Well-defined star-shaped calcite crystals formed in agarose gels. *Chemical communications* **2003**, 1180-1181.
29. Martin, R.; Brown, P. The effects of magnesium on hydroxyapatite formation in vitro from CaHPO 4 and Ca 4 (PO 4) 2 O at 37.4 C. *Calcified tissue international* **1997**, *60*, 538-546.
30. Stanley, S.M.; Ries, J.B.; Hardie, L.A. Low-magnesium calcite produced by coralline algae in seawater of Late Cretaceous composition. *Proceedings of the National Academy of Sciences* **2002**, *99*, 15323-15326.
31. Ries, J.B. Effect of ambient Mg/Ca ratio on Mg fractionation in calcareous marine invertebrates: A record of the oceanic Mg/Ca ratio over the Phanerozoic. *Geology* **2004**, *32*, 981-984.
32. Raz, S.; Testeniere, O.; Hecker, A.; Weiner, S.; Luquet, G. Stable amorphous calcium carbonate is the main component of the calcium storage structures of the crustacean Orchestia cavimana. *The Biological Bulletin* **2002**, *203*, 269-274.
33. Folk, R.L. The natural history of crystalline calcium carbonate; effect of magnesium content and salinity. *Journal of Sedimentary Research* **1974**, *44*, 40-53.
34. Orlien, V. Utilizing High Pressure Processing to Induce Structural Changes in Dairy and Meat Products. In *Reference Module in Food Science*, Elsevier: 2017.
35. Maeno, S.; Niki, Y.; Matsumoto, H.; Morioka, H.; Yatabe, T.; Funayama, A.; Toyama, Y.; Taguchi, T.; Tanaka, J. The effect of calcium ion concentration on osteoblast viability, proliferation and differentiation in monolayer and 3D culture. *Biomaterials* **2005**, *26*, 4847-4855.